



Elevated temperature and decreased salinity both affect the biochemical composition of the Antarctic sea-ice diatom *Nitzschia lecointei*, but not increased pCO₂

Anders Torstensson^{1,4} · Carlos Jiménez² · Anders K. Nilsson^{1,3} · Angela Wulff¹

Received: 14 January 2019 / Revised: 21 July 2019 / Accepted: 23 August 2019 / Published online: 30 September 2019
© The Author(s) 2019

Abstract

Areas in western Antarctica are experiencing rapid climate change, where ocean warming results in more sea ice melt simultaneously as oceanic CO₂ levels are increasing. In this study, we have tested how increased temperature (from −1.8 to 3 °C) and decreased salinity (from 35 to 20 and 10) synergistically affect the growth, photophysiology and biochemical composition of the Antarctic sea-ice diatom *Nitzschia lecointei*. In a separate experiment, we also addressed how ocean acidification (from 400 to 1000 μatm partial pressure of CO₂) affects these key physiological parameters. Both positive and negative changes in specific growth rate, particulate organic carbon to particulate organic nitrogen ratio, chl *a* fluorescence kinetics, lipid peroxidation, carbohydrate content, protein content, fatty acid content and composition were observed when cells were exposed to warming and desalination. However, when cells were subjected to increased pCO₂, only F_v/F_m , non-photochemical quenching and lipid peroxidation increased (by 3, 16 and 14%, respectively), and no other of the abovementioned biochemical properties were affected. These results suggest that changes in temperature and salinity may have more effects on the biochemical composition of *N. lecointei* than ocean acidification. Sea-ice algae are important component of polar food webs, and their nutritional quality may be affected as a result of altered environmental conditions due to climate change and sea ice melt.

Keywords Temperature · Salinity · pCO₂ · Fatty acids · TBARS · PUFA

Introduction

Sea-ice algae can contribute to up to 25% of the annual primary production in ice-covered waters, and can provide an important food source for grazers, especially in the early spring (Horner and Schrader 1982; Lizotte 2001; Arrigo and Thomas 2004). As the sea ice is melting during the summer

months, diatoms are exposed to large variations in abiotic factors (such as salinity, irradiance and nutrient levels), and are ultimately dispersed into the underlying surface water, and can potentially seed the pelagic bloom under favorable conditions (Lizotte 2001; Riaux-Gobin et al. 2011). The community composition, growth and photosynthetic activity of sea-ice microorganisms are closely related to many abiotic factors, such as nutrients, temperature, salinity, irradiance quantity and quality (Palmisano et al. 1987; Zhang et al. 1999; Rajanahally et al. 2015; Torstensson et al. 2015a). Many psychrophilic diatom taxa have evolved in the Southern Ocean (Wulff et al. 2009), and changes in environmental conditions due to predicted climate change may have fundamental consequences for several Antarctic ecosystems.

As global air and ocean temperatures continue to increase, the physicochemical properties of polar environments are shifting rapidly, especially in the Arctic and in areas around the Antarctic peninsula, where temperature has increased by > 1 °C since the 1950s (Meredith and King 2005). For instance, as the areal extent and thickness of sea

✉ Anders Torstensson
anders.torstensson@ebc.uu.se

¹ Department of Biological and Environmental Sciences, University of Gothenburg, Göteborg, Sweden

² Department of Ecology, Faculty of Sciences, University of Málaga, Málaga, Spain

³ Section for Ophthalmology, Department of Clinical Neuroscience, Institute of Neuroscience and Physiology, Sahlgrenska Academy, University of Gothenburg, Göteborg, Sweden

⁴ Department of Ecology & Genetics, Limnology, Uppsala University, Uppsala, Sweden

ice diminish leading to increased irradiance below sea ice (Arrigo et al. 2013), the extent and duration of ice features associated with salinity extremes—e.g. freshwater melt ponds, under-ice melt lenses—also increase. These factors are key components in determining the productivity and community structure of sea-ice associated and under-ice blooming microorganisms (Arrigo et al. 2012; Assmy et al. 2013; Torstensson et al. 2015a), and the melting season has been shown to be important for the development of sea-ice associated microbial communities in the Arctic (Assmy et al. 2013; Fernández-Gómez et al. 2018). Simultaneously as the global oceans become warmer, the oceanic uptake of anthropogenic CO₂ is shifting the marine carbonate system towards a less alkaline state (ocean acidification), often causing substantial changes in marine food web dynamics (Hoegh-Guldberg and Bruno 2010). The average oceanic pH is predicted to decrease by ~0.3 units by the end of the century according to IPCC RCP8.5 (IPCC 2013), and is believed to have the greatest impacts in cold environments as CO₂ dissolves more readily and there is a naturally low concentration of carbonate ions in polar oceans.

Previous work indicate that most Antarctic diatoms have an optimal growth temperature between 2 and 6 °C (Longhi et al. 2003; Schlie and Karsten 2016), and have salinity growth and photosynthesis ranges between 5 and 50 (Schlie and Karsten 2016; Torstensson et al. 2018). The reports of ocean acidification effects on sea-ice microalgae are mixed with positive, negative and unchanged responses, and most effects of moderate pCO₂ levels on the growth rate of sea-ice microorganisms are minor (reviewed in McMinn 2017). However, other biogeochemically important physiological changes may be greater in response to ocean acidification, such as carbon metabolism and nutrient uptake rates (Torstensson et al. 2015b; Qu et al. 2017). Although it has been shown that the food quality of sea-ice algae reduces as a result of increased irradiance as the sea ice become thinner (Leu et al. 2010), few studies have described how the biochemical composition of sea-ice diatoms are affected by temperature, salinity and pCO₂. These factors could potentially have significant consequences for the nutritional value of diatoms and therefore impact higher trophic levels in the Antarctic ecosystem.

As the reports of effects of climate change on sea-ice microalgae are still few (e.g. ocean acification, McMinn 2017), there is an urgent need to develop a better understanding of how these organisms will be affected by these changes in the Southern Ocean. There is also an emerging field of using cold-adapted microalgal strains as suitable candidates for commercial algal production in colder climates (Suzuki et al. 2019), which calls for baseline information about optimal growth conditions and production yields in psychrophilic microalgal cultures. In this work, we have addressed the physiological performance and biochemical composition

of the sea-ice diatom *Nitzschia lecointei* (isolated from western Antarctica), present in Southern Ocean pack ice and water column (Ligowski 1992; Ryan et al. 2004; Riaux-Gobin et al. 2011), when exposed to factors related to the melting of sea ice, such as increased temperature, lowered salinity and increased pCO₂. In two laboratory experiments, the effect of increased pCO₂ (400 and 1000 µatm) and the interaction effects of increased temperature (from –1.8 to 3 °C) and reduced salinity (35, 20 and 10) have been studied. The changes in temperature and pCO₂ represent changes that are projected to occur within the next century according to global models (IPCC 2013), and the salinity range was chosen to represent the shifts that microalgae naturally experience in Antarctic pack ice during the melting season (Torstensson et al. 2018). We hypothesized that *N. lecointei* would change in biochemical composition (carbohydrate, protein, fatty acid, particulate organic carbon [POC] and nitrogen [PON] content) in response to the treatments, even when growth rate or photosynthesis was unaffected. We also hypothesized that cells would be more prone to oxidative stress under sub-optimal growth conditions, resulting in a higher degree of lipid peroxidation.

Materials and methods

Temperature and salinity experiment

The diatom *N. lecointei* was isolated from sea ice collected in the Amundsen Sea, and was cultured at –1.8 °C and salinity 34 until the experiment started. The combined effect of increased temperature and decreased salinity was studied in an orthogonal experimental design. The original culture was split up and gradually diluted with f/2 medium (Guillard 1975) prepared from artificial seawater with three different salinities (Instant Ocean®, Spectrum Brands Inc., Blacksburg, VA, USA) until the targeted salinities were reached (10, 20 and 35). Dilutions were performed in five steps during 22 h, each step representing an approximate decrease of 3 and 5 salinity units in the intermediate and low salinity treatment, respectively. This rate was chosen to simulate natural changes that could occur when the ice is melting as described in Lyon et al. (2016). At the last step (day 0), the experiment was initiated by dividing the cultures into two water baths at different temperatures (–1.8 and 3 °C), creating six treatment groups ($n=3$). The experiment was conducted for 7 days under an 18:6 h light:dark cycle at 30 µmol photons m⁻² s⁻¹ of photosynthetic active radiation (PAR 400–700 nm), provided by fluorescent tubes (GE Polyflux XLR 18 W/860). The duration of the experiment was chosen to limit nutrient depletion and stationary growth, but long enough to have detectable growth in the more extreme treatments.

The irradiance level was measured in the water baths, and was chosen based on the light saturation parameter (E_k) of the starting culture. The positions of the flasks were rotated daily to ensure equal irradiance. Temperature was monitored throughout the experiment using HOBO Pendant data loggers (Onset Computer Corp., Pocasset, MA, USA).

CO₂ enrichment experiment

N. lecointei was inoculated in f/2 medium prepared from natural seawater (salinity 32, pre-equilibrated to 400 and 1000 μatm ($\pm 10\%$) pCO₂ by aeration of air/CO₂ mixes. CO₂ mixing was performed in-line with pure CO₂ gas (Air liquide) and 0.2 μm filtered, partially CO₂-scrubbed (Ca(OH)₂ and NaOH) indoor air. The individual culture flasks were bubbled with the air/CO₂ mixes throughout the experiment, and pCO₂ levels were monitored daily by measurements with an AirSense 310e CO₂ sensor (Digital Control Systems Inc, Portland, USA). The increase in total alkalinity (A_T) due to addition of silica was counterbalanced by the addition of 0.1 M HCl to return to realistic A_T values. The culture flasks ($n=5$ per treatment) were randomly placed in a water bath controlling the temperature at -1.8 °C and the cells were pre-acclimated to the experimental conditions for 3 days before the experiment started. The experiment lasted for 6 days and temperature was monitored throughout the experiment using HOBO Pendant data loggers (Onset Computer Corp., Pocasset, MA, USA). The experiment was conducted under an 18:6 h light:dark cycle at 30 $\mu\text{mol photons m}^{-2} \text{s}^{-1}$ of PAR, provided by fluorescent tubes (GE Polylux XLR 18 W/860).

Samples for carbonate system determination were taken every third day of the experiment, thermostated to 25 °C and pH was measured on the total scale (pH_T), using a Crison 50 10 T pH electrode (Crison Instruments, Barcelona, Spain). The electrode was calibrated daily with a Tris-HCl buffer prepared from artificial seawater with salinity 35, and pH was calculated according to Dickson et al. (2007). A_T was measured by manual potentiometric titration in an open cell with 0.02 M HCl. The equivalence point was evaluated using the Gran function (Gran 1952). The accuracy for A_T data was checked (99.4%) and calibrated against analyzed certified reference material (CRM), provided by Andrew G. Dickson, Scripps Institute of Oceanography, CA, USA. The CRM was titrated in triplicates with a standard deviation of 6 $\mu\text{mol kg}^{-1}$. Parameters of the carbonate system was calculated at in situ conditions (salinity, temperature, pressure) from measured values of pH_T, A_T , salinity and temperature using the program CO2SYS (Pierrot et al. 2006). K_1 and K_2 constants used in calculations were determined by Mehrbach

et al. (1973) and refitted by Dickson and Millero (1987). The constant for SO₄⁻ was determined by Dickson (1990).

Cell density and growth rate

Diatom cell density was counted in live samples using a BD Accuri C6 flow cytometer (BD Biosciences, San Jose, CA, USA) until a minimum of 2000 cells per sample were counted. No signs of aggregation or biofilm formation were observed in the cultures, and cell abundances were maintained within the range that can occur in sea ice throughout the experiment (Arrigo 2017). Samples were analyzed daily for the salinity and temperature experiment, and every third day for the CO₂ enrichment experiment. Growth curves were log-transformed and modeled using a spline fit in the R package growthrates (Petzoldt 2018; R Core Team 2018), and the maximum specific growth rate (μ_{max}) was calculated from the model's first derivative (Kahm et al. 2010).

Variable fluorescence

The photosynthetic performance of *N. lecointei* was analyzed by rapid light curves (RLC) using PAM-fluorometry (Water-PAM, Universal control unit, Water-ED, Walz Mess- und Reigeltechnik, Effeltrich, Germany) (Ralph and Gademann 2005). The Water-ED unit was kept on ice in a temperature-controlled room set to 2 °C during all measurements. Cells were dark adapted for a minimum of 30 min, which was verified to be sufficient by multiple maximum quantum yield (F_v/F_m) measurements over the course of one hour prior to the start of the experiments. The F_v/F_m and effective quantum yield (ϕ_{PSII}) of photosystem II (PSII) were measured by applying a low level of light to determine minimum fluorescence (F_0 and F) and the maximum fluorescence (F_m and F_m') by exposing the sample to a short saturation pulse of measuring light ($> 3000 \mu\text{mol photons m}^{-2} \text{s}^{-1}$ for 0.8 s). Variable fluorescence ($F_v = F_m - F_0$) and F_v/F_m were determined for all samples prior to the start of RLCs. RLCs were performed by measurement of ϕ_{PSII} ($(F_m' - F)/F_m'$) of quasi-adapted (15 s) cells to stepwise increasing actinic light levels in the Water-PAM measuring unit (0, 29, 45, 63, 96, 143, 219, 322 and 492 $\mu\text{mol photons m}^{-2} \text{s}^{-1}$, as calibrated with a WALZ Micro Quantum Sensor US-SQS/IB). The relative electron transport rate (rETR) was then calculated as $\text{rETR} = \phi_{\text{PSII}} \times \text{PAR}$, where PAR is the irradiance in $\mu\text{mol photons m}^{-2} \text{s}^{-1}$. The saturating rETR-RLCs were fitted using Eilers and Peeters (1988), so that E_k ($\mu\text{mol photons m}^{-2} \text{s}^{-1}$), the photosynthetic efficiency as the initial slope (α_{PSII}) and the relative maximum ETR (rETR_{max}) were calculated. Non-photochemical quenching (NPQ) describes regulated dissipation of excess energy and the capacity of protection of the photosynthetic electron transport chain,

and it was determined in a separate sample after exposure of $96 \mu\text{mol photons m}^{-2} \text{s}^{-1}$ for 210 s, and calculated by $(F_m - F'_m)/F'_m$ (Ralph and Gademann 2005).

Total carbohydrates

The samples for total carbohydrates (10–40 mL) were collected on Whatman GF/F filters by gentle filtration (0.2 bar) and subsequently stored at -20°C until further processing. Samples were extracted in distilled water while sonicated using a UP50H sonicating probe (Hielscher Ultrasonic GmbH, Teltow, Germany) operating at 80% for 30 s. The samples were heated to 80°C for 2 hours and centrifuged for 10 min at $14,000\times g$ to remove cell debris. Total carbohydrates were measured in the supernatant using the phenol–sulphuric acid method (Kochert 1978). In brief, a sample (1.5 mL) was mixed with 50 μL 80% phenol and 5 mL H_2SO_4 and left to react for 30 min. The absorbance of the sample was read at 485 nm and carbohydrate concentration was calculated using glucose as standard.

Total proteins

Cells (100–300 mL culture) were harvested by centrifugation (7 min at $3000\times g$, 4°C), and frozen in liquid nitrogen. Samples were stored at -80°C until extraction of proteins. Proteins were extracted by adding 100 μL of 10% SDS on frozen biomass and homogenized in a Retsch MM400 mixer mill (Retsch, Haan, Germany). Samples were sonicated on ice using a UP50H sonicating probe (Hielscher Ultrasonic GmbH, Teltow, Germany) operating at 80% for 30 s and subsequently mixed with 400 μL of lysis buffer (50 mM β -glycerophosphate pH 7.2, 0.1 mM sodium vanadate, 2 mM MgCl_2 , 1 mM EGTA, 1 mM dithiothreitol, 2 $\mu\text{g mL}^{-1}$ leupeptin and 4 $\mu\text{g mL}^{-1}$ aprotinin). A second sonication step was applied for 30 s, and samples were finally centrifuged for 30 min at 4°C and $14,000\times g$ to remove cell debris. Proteins from the supernatant were concentrated using Pall Nanosep® 10 K Centrifugal devices (Pall Corporation, Michigan, USA) and quantified according to the bicinchoninic acid method (Smith et al. 1985), using bovine serum albumins (Sigma-Aldrich, Madrid, Spain) as standard.

Lipid extraction and fatty acid analysis

A well-mixed sample (15–50 mL) was filtered onto pre-combusted (4 h at 450°C) Whatman GF/F (Whatmann, Merck KGaA, Darmstadt, Germany) filters, flash frozen in liquid nitrogen and stored at -80°C until further processing. For lipid extraction, the frozen filters were spiked with 5 μg of the internal standard di-nonadecanoyl phosphatidylcholine (Larodan, Solna, Sweden) and boiled in 2-propanol for 5 min. Samples were evaporated to dryness under N_2 flow

at 40°C . Fatty acids from glycerolipids were derivatized to fatty acid methyl esters (FAMES) by direct alkaline trans-methylation through the addition of 1 mL of 0.5 M sodium methoxide and 250 μL of heptane and sonication for 30 min. Samples were acidified with 50 μL of acetic acid and diluted with 1 mL of distilled water. After thorough vortex-mixing, samples were centrifuged and the upper organic phase collected, evaporated under N_2 flow, and finally the dried residue was dissolved in 30 μL acetonitrile. 1 μL of the sample was used for analysis on an Agilent 7820 gas chromatograph coupled to an Agilent 5975 mass selective detector (Agilent Technologies, Santa Clara, USA) as described in Nilsson et al. (2019). The mass detector was operated in scan mode (m/z 50–400) and total ion chromatograms from FAMES were integrated and quantified using MassHunter Work Station Software Quantitative Analysis for GCMS (Version B.06.00, Agilent Technologies, Santa Clara, USA).

Particulate organic carbon and nitrogen

A well-mixed sample (15–50 mL) was filtered onto pre-combusted (4 h at 450°C) Whatman GF/F filters. The filters were rinsed with distilled water to remove salts, and subsequently stored at -20°C until further processing. Samples were dried at 60°C during 48 h. The filters were fumigated with 10% HCl for 4 h to remove inorganic carbon and analysis of particulate organic carbon (POC) and nitrogen (PON) was performed with a PerkinElmer 2400 CHN Elemental Analyzer at 950°C .

Lipid peroxidation

Oxidative stress in the cellular environment results in the formation of highly reactive and unstable lipid hydroperoxides. Decomposition of the unstable peroxides derived from PUFAs results, among others, in the formation of thiobarbituric acid reactive substances (TBARS) as by-products of lipid peroxidation (i.e. as degradation products of lipids), which can be detected by the TBARS assay using thiobarbituric acid as reagent.

Cells were collected by gentle filtration (0.2 bar) on Millipore 0.8 μm ATTP Isopore membrane filters and immediately frozen in liquid nitrogen, and subsequently stored at -80°C . Samples were analyzed using a method of Heath and Packer (1968), modified by van de Poll et al. (2006). In brief, 0.8 mL MilliQ was added to frozen biomass followed by an ultrasonic extraction using a Vibra-cell sonicating probe, operating at 80% in 5-s pulses. After sonication, 0.8 mL of 0.5% (w/v) thiobarbituric acid in 20% (w/v) trichloroacetic acid was added and samples were incubated at 90°C for 30 min. Samples were put on ice and filtered through a 0.45 μm nylon filter. Absorbance was measured at 532 and 600 nm on a Shimadzu UV-1800 spectrophotometer, using

extraction solvent as blank. The amount of TBARS was calculated using an extinction coefficient of $155 \text{ mM}^{-1} \text{ cm}^{-1}$, and expressed as malondialdehyde equivalents.

Statistical analysis

Longitudinal data were analyzed using linear mixed effect (LME) models using the nlme package in R (Pinheiro et al. 2018; R Core Team 2018). The models were fitted using the interaction between pCO₂ concentration and Day, where both were treated as fixed factors. The individual sample flask was included as a random factor (random intercept) in the model to account for repeated measurements over time, using a compound symmetry covariance structure. Parametric assumption were assured by graphical exploration of the data (Quinn and Keough 2002). Student's *t* tests were used to test differences between pCO₂ in non-longitudinal data, and two-way ANOVA was used for testing the interaction between temperature and salinity. Tukey's HSD test was used to explore differences over time and between treatments. Statistical significance was determined using a probability level of <0.05 .

Results

Effects of increased temperature and decreased salinity

Growth rate

The maximum specific growth rate of *N. lecointei* was significantly affected by the interaction between temperature and salinity ($p < 0.01$, $F_{2,12} = 11.2$, two-way ANOVA, Fig. 1a), where rates were faster at 3 °C compared to -1.8 °C (Fig. 1a). All treatments were significantly different ($p < 0.0001$, Tukey's test) except for salinity 20 and 35 both at -1.8 °C ($p = 0.999$, Tukey's test) and at 3 °C ($p = 0.0664$, Tukey's test). Cell density increased between 5 and sixfold during the 7 days of cultivation at 3 °C and salinity 35 and 20, respectively, while it only increased 2.5 times at -1.8 °C at the same salinities. Maximal cell density after 7 days of cultivation reached 1.9×10^5 cells mL⁻¹ at 3 °C, while only 0.9×10^5 cells mL⁻¹ were counted at -1.8 °C. At both temperatures, growth was limited at salinity 10.

Biochemical composition

Cellular carbon content was in general higher at the beginning than at the end of the experiment (Table 1). In addition, carbon content was significantly higher at -1.8 °C than at 3 °C ($p < 0.0001$, $F_{1,12} = 103$, two-way ANOVA) and was affected by salinity ($p < 0.0001$, $F_{2,12} = 151$,

two-way ANOVA) after 7 days of cultivation. Here, carbon cell content was highest at salinity 10, and lowest at salinity 20 ($p < 0.0001$, Tukey's test). Cellular nitrogen content (Table 1) was synergistically affected by temperature and salinity ($p < 0.001$, $F_{2,12} = 103$, two-way ANOVA), where nitrogen content was higher at low temperature in the salinity 10 treatment ($p < 0.001$, Tukey's test), but not affected by temperature at salinity 20 and 35 ($p = 0.82$, Tukey's test). The nitrogen content was significantly higher at salinity 10 compared to salinity 20 and 35 ($p < 0.0001$, Tukey's test). These changes in C and N content induced small differences in the C/N ratio (Fig. 1b; Table 1): first, it was always higher at day 0; second, it was higher at -1.8 °C than at 3 °C ($p < 0.0001$, $F_{1,12} = 101$, two-way ANOVA); third, it was also significantly affected by salinity ($p = 0.00108$, $F_{2,12} = 12.7$, two-way ANOVA), being lower at salinity 20 compared to 35 ($p < 0.001$, Tukey's test).

The content of carbohydrates showed some variations during growth; the main difference between treatments was that carbohydrate content was affected by salinity ($p = 0.0008$, $F_{2,12} = 13.8$, two-way ANOVA, Fig. 1c), being lower at salinity 20 than at salinity 10 and 35 ($p < 0.002$, Tukey's test). In addition, carbohydrate content was significantly reduced by temperature, and cells accumulated more carbohydrates at -1.8 °C than at 3 °C ($p < 0.0001$, $F_{1,12} = 36.2$, two-way ANOVA). Protein content showed the reverse scenario, being maximal at 3 °C and salinity 20 after 7 days of cultivation ($p = 0.003$, $F_{1,12} = 13.8$, two-way ANOVA, Fig. 1d), i.e. at the optimal temperature and salinity conditions for the growth of *N. lecointei*.

The cellular fatty acid content was also affected both by temperature and salinity ($p < 0.0001$, $F_{1,12} = 99.3$ and $F_{2,12} = 162$, respectively, two-way ANOVA, Fig. 1e). Cells had higher fatty acid content at -1.8 °C compared to 3 °C, and at salinity 10 compared to 20 and 35 ($p < 0.0001$, Tukey's tests). There was no significant difference between salinity 20 and 35 ($p = 0.19$, Tukey's test).

TBARS, which indicate the degree of lipid peroxidation in cells, were very similar (not statistically significant) directly after acclimation for all treatments (data not shown), while significant differences appeared after 7 days (Fig. 1f). Both temperature and salinity had significant effects on TBARS content ($p < 0.0001$ and $p = 0.012$, $F_{2,10} = 29.6$ and $F_{1,10} = 9.4$, two-way ANOVA), where salinity 10 had higher TBARS content than 20 and 35 ($p < 0.001$, Tukey's test). TBARS content was also lower at high temperature, although data are missing for salinity 10 at -1.8 °C due to insufficient biomass for analysis (Fig. 1f). Salinity 10 at 3 °C seemed to induce the highest oxidative stress to *N. lecointei*, also resulting in a decrease of growth.

Fatty acid profiles of cells grown at both 3 °C and -1.8 °C displayed a clear salinity dependent separation at 7 days of cultivation in a two-dimension non-metric

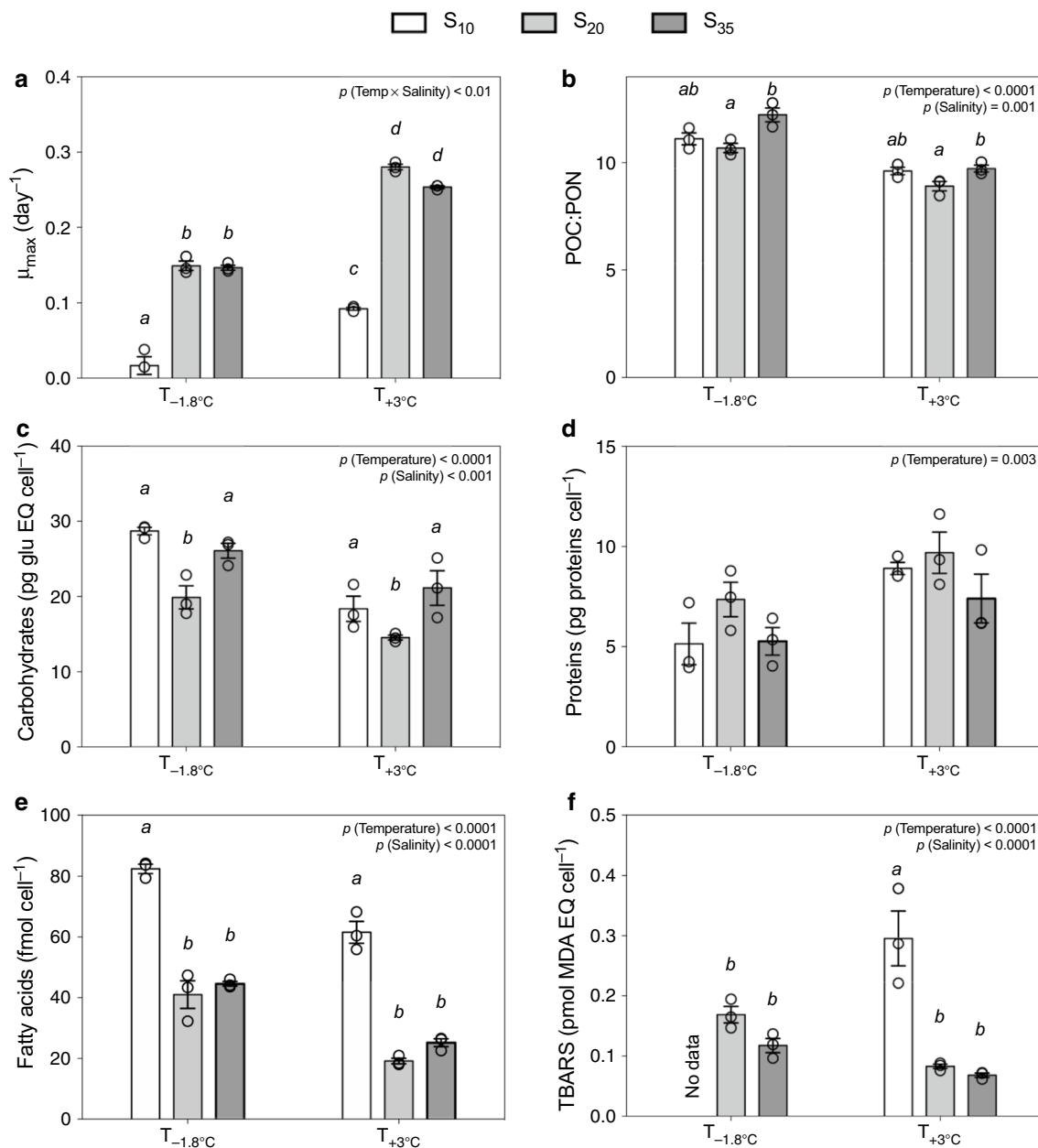


Fig. 1 Growth and biochemical composition of *Nitzschia lecontei* cells after 7 days exposure to a combination of temperature (−1.8 and 3 °C) and salinity (10, 20 and 35) treatments. Listed parameters are **a** maximum specific growth rate (μ_{max}), **b** POC:PON ratio, **c** carbohydrate **d** protein and **e** fatty acid content, and **f** cellular thiobarbituric acid reactive substances (TBARS) content, expressed in malondialdehyde equivalents (MDA EQ). Error bars represent standard error,

and the individual values are displayed with open circles ($n=3$). p values of the ANOVA models are listed when statistically significant ($p < 0.05$). Italic letters indicate statistical significance ($p < 0.05$, Tukey's test) between all groups when a significant interaction was present (**a**) and between salinity treatments when the main salinity effect was statistically significant (**b**, **c**, **e** and **f**)

multidimensional scaling plot (Fig. 2). There were significant interactions between temperature and salinity in the total molar fraction of polyunsaturated fatty acids (PUFAs) and monounsaturated fatty acids (MUFAs) ($p < 0.01$, $F_{2,12} = 7.1$ and 28.6, respectively, two-way ANOVAs). For cells grown at −1.8 °C, there was a difference in molar fraction of PUFAs between cells grown at salinity

10 and those grown at 20 or 35 ($p < 0.03$, Tukey's tests, Fig. 3), but there were no differences between the salinities in MUFA content ($p > 0.58$, Tukey's test, Fig. 3). Similarly, cells grown at 3 °C showed significant differences in PUFA and MUFA content in all three salinity levels ($p < 0.05$, Tukey's tests, Fig. 3).

Table 1 Carbon and nitrogen content in *Nitzschia lecoointei* after 7 days of exposure to a combination of increased temperature and reduced salinity

Day	7															
	-1.8				3				-1.8				3			
	35	20	10	35	20	10	35	20	10	35	20	10	35	20	10	
POC:PON	15.2 (1.3)	12.6 (0.3)	12.5 (0.6)	12.4 (0.6)	12.4 (0.4)	12.5 (0.5)	12.4 (0.3)	12.2 (0.6)	10.7 (0.4)	11.1 (0.5)	11.1 (0.5)	11.1 (0.5)	9.7 (0.3)	8.9 (0.4)	9.6 (0.3)	
C (pg cell ⁻¹)	120.3 (12.8)	98.3 (3.2)	92.4 (7.9)	94.3 (3.2)	94.4 (3.1)	89.2 (5.4)	89.2 (5.4)	67.0 (0.9)	59.0 (0.2)	105.2 (1.8)	105.2 (1.8)	105.2 (1.8)	56.7 (4.9)	50.7 (3.1)	72.6 (6.3)	
N (pg cell ⁻¹)	9.2 (0.2)	9.1 (0.5)	8.6 (0.4)	8.9 (0.2)	8.8 (0.1)	8.4 (0.4)	8.4 (0.4)	6.4 (0.4)	6.4 (0.2)	11.1 (0.5)	11.1 (0.5)	11.1 (0.5)	6.8 (0.4)	6.6 (0.2)	8.8 (0.5)	

Day 0 show data 1 h after a 22-h gradual dilution to the respective salinity (see "Methods" for details). Averages and standards deviation are shown ($n=3$)

The total fraction of saturated fatty acids (SFAs) in cells was significantly higher in cells grown at salinity 10 compared to 35 and 20 ($p < 0.0001$, Tukey's tests, Table 2), but there was no difference between 35 and 20 ($p = 0.86$, Tukey's test, Table 2). Cells also had a higher fraction of SFAs at -1.8 °C compared to 3 °C ($p < 0.03$, $F_{1,12} = 6.8$, two-way ANOVA, Table 2). In addition, fatty acid chain length was not influenced by temperature or salinity as determined by the Chain Length Index (Mocking et al. 2012, data not shown).

Fluorescence measurements

There was a significant effect of temperature, salinity, and the interactions between temperature and salinity, temperature and day, salinity and day on F_v/F_m in *N. lecoointei* (Table 3, Fig. 4a). There was a temporal decrease in F_v/F_m for both salinity 10 and 35 at -1.8 °C during the first 3 days of experiment (Fig. 4a), whereas cells in salinity 20 had more stable F_v/F_m throughout the experiment. F_v/F_m was generally higher at 3 °C compared to -1.8 °C (Fig. 4a).

The RLC-derived parameters ($rETR_{max}$, α_{PSII} and E_k) were significantly affected by the treatments in different ways. $rETR_{max}$ was affected by all interactions and main effects (Table 3), where the rate was generally lowest and with stable levels throughout the experiment at salinity 35 (Fig. 4b). For salinity 10, however, $rETR_{max}$ gradually increased at both temperatures (Fig. 4b). Cells in the intermediate salinity level (20) expressed different temporal behaviors at the two temperatures, where it was gradually increasing at -1.8 °C while maintained stable at 3 °C (Fig. 4b). α_{PSII} was generally higher at 3 than at -1.8 °C, indicating higher efficiency of the photosynthesis at low irradiance at the highest temperature (Fig. 4c; Table 3). However, salinity had a negative effect on α_{PSII} at 3 °C, a pattern not observed at -1.8 °C (Fig. 4c; Table 3). E_k was initially high in cells treated with salinity 20 and 3 °C, but decreased after 2 days of experiment (Fig. 4d). However, an opposite pattern was observed in the same salinity treatment at -1.8 °C, where E_k increased after 3 days (Fig. 4d). Cells in the remaining treatments had a stable E_k throughout the experiment (Fig. 4d).

Finally, NPQ was affected by all treatments and interactions, except for the interaction between temperature and salinity (Table 3). Initially, NPQ was high in both salinity 20 treatments, but decreased already after one day (Fig. 4e). NPQ was always lowest in salinity 35 at -1.8 °C (Fig. 4e). At 3 °C, NPQ gradually decreased in cells grown at salinity 35, whereas it increased in salinity 20 and 10 after 3 days (Fig. 4e).

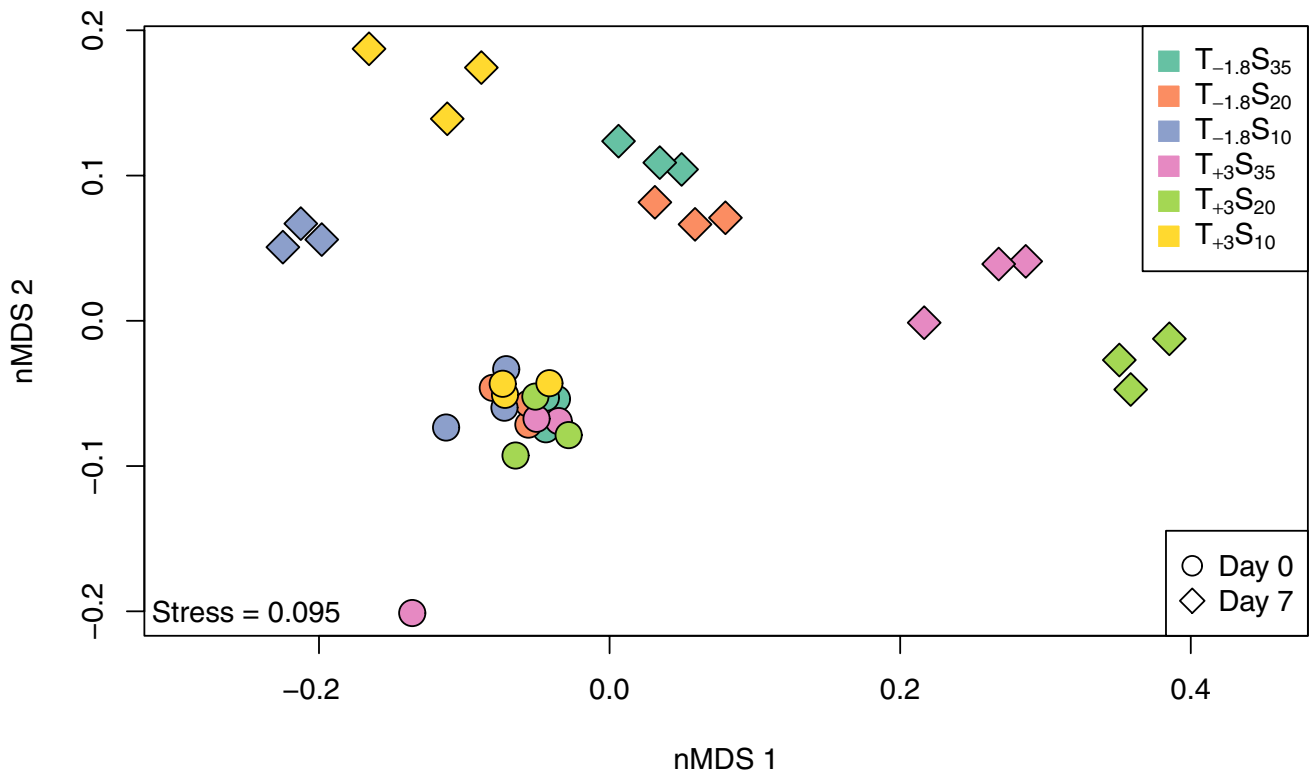


Fig. 2 Non-metric multidimensional scaling over the fatty acid composition of *Nitzschia lecointei* exposed to a combination of increased temperature and decreased salinity, based on Bray–Curtis dissimilar-

ity. Day 0 shows fatty acid data 1 h after a 22-h gradual dilution to the respective salinity (see “Methods” for details). The detailed composition of fatty acids is presented in Table 2

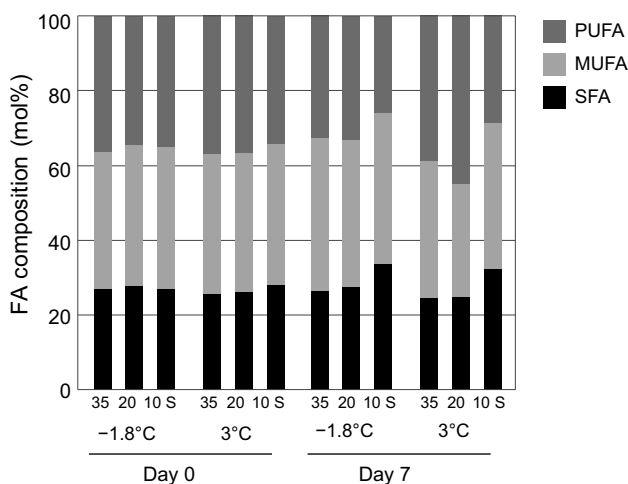


Fig. 3 Average molar composition (%) of the fatty acids groups polyunsaturated fatty acids (PUFA), monounsaturated fatty acids (MUFA) and saturated fatty acids (SFA) in *Nitzschia lecointei* during the temperature and salinity experiment

Effects of CO₂ enrichment

Carbonate system

The carbonate system parameters during the cultivation period are shown in Table 4. CO₂ concentration in the air introduced to the cultures was set around 400 and 1000 μatm; however, real concentration in the cultures was slightly lower, reaching values representing the actual and future pH of the seawater according to the expected increase of atmospheric CO₂ within the next century. As a consequence of the enrichment with CO₂, pH_T of the cultures changed, reaching values of 8.10 and 7.69 in the 400 and 1000 μatm treatment, respectively (Table 4).

Growth rate

Increased CO₂ concentration did not have any influence on the growth of *N. lecointei* ($p=0.51$, t test, $t_8=-0.70$, Table 5). Cell concentration increased from values around 0.6×10^5 to 2.6×10^5 cells mL⁻¹ in 6 days.

Table 2 Molar percent of individual fatty acids

Experiment	Temperature and salinity												CO ₂	
	Ambient												400	1000
pCO ₂ (µatm)														
Cultivation time (days)	7												6	
Temperature (°C)	3			-1.8			3			-1.8				
Salinity	35	20	10	35	20	10	35	20	10	35	20	10	32	
14:0	12.7 (1.1)	12.7 (1.8)	11.5 (3.9)	10.8 (4.9)	11.5 (2.1)	13.2 (1.0)	9.7 (1.0)	9.8 (3.9)	12.1 (0.8)	9.0 (1.5)	11.5 (1.3)	13.6 (1.2)	10.2 (2.1)	9.6 (2.6)
16:0	11.6 (0.4)	12.2 (0.3)	12.3 (0.7)	11.9 (0.9)	11.8 (0.8)	12.0 (0.6)	13.9 (0.8)	13.9 (0.8)	17.7 (0.5)	13.5 (0.5)	11.5 (0.8)	15.5 (0.8)	10.0 (1.0)	9.9 (2.1)
16:1 <i>n</i> -7	33.7 (1.1)	34.5 (1.2)	34.7 (0.8)	33.8 (0.5)	33.8 (1.5)	34.7 (0.8)	37.7 (0.7)	36.0 (0.9)	36.8 (0.3)	32.5 (0.9)	25.4 (1.4)	35.3 (1.5)	25.0 (1.9)	23.3 (3.4)
16:2	2.0 (0.0)	2.0 (0.1)	2.0 (0.0)	1.9 (0.1)	2.0 (0.0)	2.0 (0.0)	2.1 (0.1)	2.0 (0.1)	1.6 (0.0)	3.3 (0.1)	4.0 (0.3)	1.5 (0.1)	3.2 (0.1)	3.0 (0.2)
16:3 <i>n</i> -4	1.3 (0.1)	1.2 (0.1)	1.2 (0.1)	1.2 (0.1)	1.2 (0.1)	1.2 (0.1)	2.6 (0.2)	3.0 (0.1)	1.2 (0.1)	5.0 (0.1)	7.9 (0.2)	2.1 (0.2)	5.7 (0.3)	5.8 (0.9)
16:4 <i>n</i> -4	7.6 (0.2)	6.9 (0.4)	6.3 (0.6)	7.0 (1.2)	7.0 (0.4)	6.6 (0.2)	6.1 (0.5)	6.9 (0.5)	4.7 (0.2)	9.1 (0.1)	11.1 (0.2)	3.9 (0.4)	14.1 (1.6)	14.2 (2.3)
18:0	2.3 (0.0)	2.5 (0.1)	2.7 (0.4)	2.6 (0.7)	2.4 (0.2)	2.4 (0.2)	2.5 (0.2)	3.2 (0.7)	3.4 (0.3)	1.8 (0.0)	1.3 (0.1)	2.5 (0.2)	0.6 (0.1)	0.8 (0.3)
18:1 <i>n</i> -9	0.4 (0.0)	0.4 (0.1)	0.4 (0.1)	0.4 (0.1)	0.4 (0.0)	0.4 (0.0)	0.4 (0.0)	0.3 (0.1)	0.3 (0.1)	0.3 (0.1)	0.2 (0.0)	0.6 (0.1)	0.3 (0.0)	0.3 (0.1)
18:1 <i>n</i> -7	0.7 (0.0)	0.8 (0.1)	0.9 (0.2)	0.8 (0.1)	0.8 (0.1)	0.7 (0.1)	0.7 (0.0)	0.8 (0.1)	1.0 (0.0)	0.8 (0.0)	1.0 (0.1)	1.3 (0.1)	0.6 (0.1)	0.6 (0.1)
18:3 <i>n</i> -3	1.9 (0.1)	1.8 (0.2)	1.9 (0.2)	2.0 (0.2)	1.9 (0.1)	1.7 (0.1)	4.5 (0.1)	2.6 (0.2)	1.9 (0.1)	3.8 (0.1)	3.2 (0.3)	3.8 (0.1)	1.5 (0.2)	1.4 (0.2)
18:4 <i>n</i> -3	9.9 (0.3)	9.6 (0.7)	10.1 (1.3)	10.6 (1.3)	9.9 (0.7)	9.1 (0.3)	8.2 (0.4)	9.3 (1.0)	8.0 (0.2)	6.3 (0.5)	6.9 (0.6)	7.7 (0.2)	9.8 (0.8)	9.9 (1.2)
20:5 <i>n</i> -3	11.7 (1.6)	11.3 (1.2)	12.0 (1.8)	12.4 (2.9)	12.7 (1.7)	12.2 (0.9)	7.7 (0.7)	7.6 (2.0)	7.6 (0.6)	9.1 (0.6)	9.0 (1.8)	8.3 (1.9)	12.8 (5.0)	15.0 (11.2)
22:6 <i>n</i> -3	1.3 (0.1)	1.1 (0.1)	0.9 (0.1)	1.2 (0.2)	1.2 (0.1)	0.9 (0.1)	0.9 (0.2)	1.2 (0.1)	0.7 (0.0)	1.4 (0.1)	1.9 (0.5)	0.8 (0.3)	2.5 (0.8)	2.3 (0.9)
24:1	1.9 (0.1)	2.1 (0.2)	2.1 (0.2)	2.4 (1.0)	2.2 (0.4)	1.9 (0.0)	2.1 (0.1)	2.5 (0.5)	2.1 (0.1)	2.9 (0.2)	3.6 (0.1)	1.9 (0.0)	2.2 (0.5)	2.2 (0.4)

Averages and standards deviation are shown (*n* = 3 and 5 for the temperature and salinity experiment and the CO₂ experiment, respectively). Day 0 show fatty acid profiles 1 h after a 22-h gradual dilution to the respective salinity (see "Methods" for details)

Table 3 Summary of three-way interactions from linear mixed effect models of the photosynthetic parameters in *Nitzschia lecointei*, after being exposed to two temperature (−1.8 and 3 °C) and three salinity (10, 20 and 35) treatments

Source of variation	df _{num}	df _{den}	F_v/F_m		rETR _{max}		α_{PSII}		E_k		NPQ	
			F	p	F	p	F	p	F	p	F	p
Temperature	1	12	265.9	<0.0001	113.396	<0.0001	165.496	<0.0001	3.545	0.0842	67.743	<0.0001
Salinity	2	12	184.8	<0.0001	272.500	<0.0001	41.726	<0.0001	47.752	<0.0001	63.200	<0.0001
Day	1	120	0.2	0.6906	34.644	<0.0001	14.649	0.0002	1.073	0.3024	28.863	<0.0001
Temperature:salinity	2	12	10.2	0.0026	5.098	0.0250	8.347	0.0054	1.259	0.3188	2.727	0.1056
Temperature:day	1	120	9.9	0.0020	8.270	0.0048	1.676	0.1980	9.478	0.0026	9.308	0.0029
Salinity:day	2	120	9.6	0.0001	10.150	0.0001	2.202	0.1151	1.437	0.2416	5.749	0.0043
Temperature:salinity:day	2	120	0.2	0.8241	18.287	<0.0001	1.025	0.3620	9.170	0.0002	5.467	0.0056

Listed parameters are maximum quantum yield of PSII (F_v/F_m), maximum relative electron transport rate (rETR_{max}), PSII efficiency (α_{PSII}), light saturation point (E_k) and non-photochemical quenching (NPQ)

Biochemical composition

POC, PON, C/N ratios, carbohydrate, protein and fatty acid content were not significantly affected by elevated pCO₂ ($p > 0.05$, t tests, Table 5). Fatty acid composition did not change by increased pCO₂ (Table 2). However, TBARS content was higher at 1000 than at 400 μatm pCO₂. Samples treated with high CO₂ had 14% higher TBARS content than in the control, indicating higher lipid peroxidation at high CO₂ ($p = 0.0085$, $t_8 = -3.5$, t test, Fig. 5).

Fluorescence measurements

Initial F_v/F_m was 0.56 in both conditions and increased during the experiment, and reached significantly higher levels at 1000 μatm compared to 400 μatm on Day 3 ($p = 0.001$, Tukey's test, Fig. 6a) and Day 6 ($p < 0.0001$, Tukey's test, Fig. 6a). Thus, there was a significant interaction between time and CO₂ concentration on F_v/F_m ($p = 0.0038$, $F_{2,16} = 8.1$, LME). For RLC-derived photosynthetic parameters, only E_k showed a similar response as F_v/F_m (Fig. 6b–d), and it was the only parameter significantly affected by high CO₂ ($p = 0.02$, $F_{1,8} = 8.2$; LME), where it was on average 16% higher in cells exposed to high CO₂. Both CO₂ concentration and time had a significant effect on NPQ ($p = 0.0220$ and 0.0023 , $F_{1,8} = 8.0$ and $F_{2,16} = 9.1$, respectively, LME). Irrespective of day, NPQ was 15% higher at elevated CO₂ (Fig. 6e). In addition, NPQ was significantly lower at Day 6 compared to Day 0 ($p = 0.007$, Tukey's test).

Discussion

This study provides insight on the physiology and biochemical composition of the Antarctic diatom *Nitzschia lecointei* when subjected to short-term environmental

stress in terms of temperature, salinity and pCO₂. These factors were used to simulate how a sea-ice diatom may respond to summer ice melt, as cells are exposed to variable salinities within sea ice (Torstensson et al. 2018), and can ultimately be exposed to projected future temperature and pCO₂ scenarios (IPCC 2013) as cells are dispersed into the water column. When cells were exposed to increased temperature (from −1.8 to 3 °C) and reduced salinity (from 35 to 20 and 10), changes in specific growth rate, POC:PON, chl *a* fluorescence kinetics, carbohydrate content, protein content, TBARS content, fatty acid content and composition were observed. However, when cells were subjected to increased pCO₂ in a separate experiment (from 400 to 1000 μatm), only minor effects were detected in chl *a* fluorescence kinetics and TBARS content, suggesting that rapid changes in temperature and salinity may have greater effects on the physiology and biochemical composition of *N. lecointei* than ocean acidification.

As *N. lecointei* grew faster and had higher photosynthetic yields at a temperature closer to its optimal growth temperature, which is around 5 °C (Torstensson et al. 2013), its biochemical composition shifted towards a lower POC:PON (closer to Redfield ratio), with higher protein content, but reduced fatty acid and carbohydrate content. Relative fatty acid composition was also affected by temperature, where cells grown at 3 °C had higher relative PUFA content (mainly hexadecatetraenoic [16:4 *n*-4], hexadecatrienoic [16:3 *n*-4] and eicosapentaenoic [20:5 *n*-3] acids) and lower relative MUFA content than cells grown at −1.8 °C. In contrast to other studies (Teoh et al. 2013), our findings suggest that the nutritional quality of our studied diatom may be higher at elevated temperature, assuming that the diatom had no nitrogen limitation in the culture medium. However, it is important to consider that the diatoms in our study was grown under nutrient-replete conditions and that other factors related to climate change, such as increased irradiance (Leu et al. 2010), may have other, and possibly

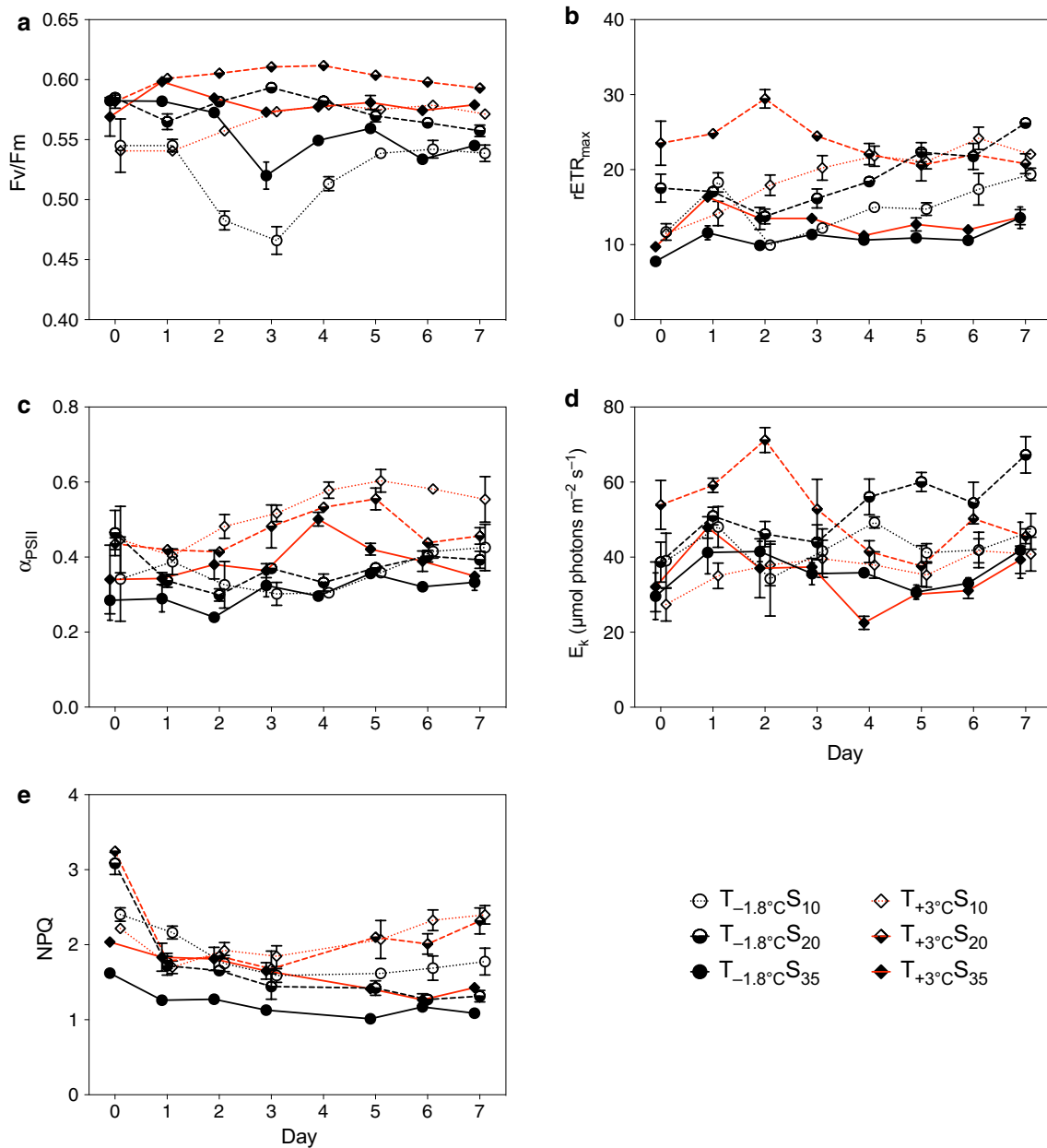


Fig. 4 Variable fluorescence parameters in *Nitzschia lecointei* after 7 days of exposure to a combination of temperature (−1.8 and 3 °C) and salinity (10, 20 and 35) treatments. Parameters included are **a** Maximum quantum yield of PSII (F_v/F_m), **b** non-photochem-

ical quenching (NPQ), **c** maximum relative electron transport rate ($rETR_{max}$), **d** PSII efficiency (α_{PSII}) and **e** light saturation point (E_k). Error bars represent standard error ($n=3$)

synergistically, effects on the nutritional quality of sea-ice algae. It is well-know that PUFAs increase membrane fluidity and thylakoid membrane functionality in diatoms (Kates and Volcani 1966), and that PUFA production is elevated at low temperature (Thomas and Dieckmann 2002). However, cells in the present study also responded by increasing the total amount of fatty acids at −1.8 °C, resulting in a higher total amount of PUFA content at low temperature even if the relative proportion of PUFA was lower. Hence, cells were

possibly compensating for the reduced growth by overproducing all fatty acids.

A field study from the Weddell Sea has suggested that decreased temperature and increased salinity impair photosynthetic capacity of sea-ice algae during ice formation (Gleitz and Thomas 1993). Although growth and F_v/F_m was drastically suppressed in *N. lecointei* at salinity 10, the chl *a* fluorescence parameters $rETR_{max}$, α_{PSII} , E_k and NPQ suggest that the PSII operated normally during the

Table 4 Arithmetic and true (pH_T) mean of carbonate system parameters at in situ temperature

Day	Treatment (μatm)	Temp ($^{\circ}\text{C}$)	Salinity	pH_T	A_T ($\mu\text{mol kg}^{-1}$)	pCO_2 (μatm)
0	400	-0.4	32	8.11	2257 (11)	326 (6)
	1000	-0.4	32	7.71	2266 (9)	884 (82)
3	400	-1.5	32	8.13	2311 (7)	315 (12)
	1000	-1.5	32	7.73	2323 (10)	840 (27)
6	400	-1.5	32	8.10	2380 (4)	349 (7)
	1000	-1.5	32	7.69	2382 (2)	976 (29)

pCO_2 was calculated from pH_T and A_T , using the K_1 and K_2 constants determined by Mehrbach et al. (1973) and refitted by Dickson and Millero (1987). The constant for SO_4^- was determined by Dickson (1990). Values in parenthesis represent standard errors ($n=5$)

Table 5 Maximum specific growth rate (μ_{max}) and biochemical composition of *Nitzschia lecointei* after 6 days of cultivation at two pCO_2

Parameter	pCO_2 (μatm)	
	400	1000
μ_{max}	0.222 (0.007)	0.226 (0.014)
POC:PON	12.3 (1.7)	11.5 (0.3)
POC (pg cell^{-1})	37.2 (5.6)	32.8 (3.6)
PON (pg cell^{-1})	3.53 (0.3)	3.33 (0.3)
Carbohydrates ($\text{pg glu EQ cell}^{-1}$)	15.5 (0.8)	16.8 (1.9)
Proteins (pg cell^{-1})	6.16 (0.5)	6.46 (1.0)
Fatty acids (fmol cell^{-1})	19.1 (1.0)	20.3 (3.6)

Values in parenthesis represent standard deviation ($n=5$)

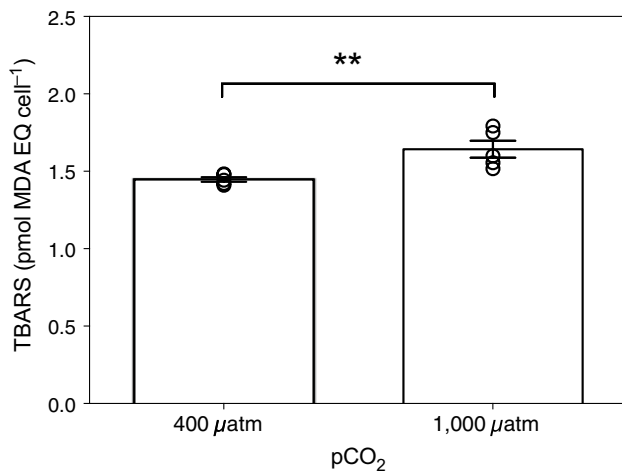


Fig. 5 Cellular thiobarbituric acid reactive substances (TBARS) content at the end of the ocean acidification experiment, expressed in malondialdehyde equivalents (MDA EQ). Error bars represent standard error and the individual values are displayed with open circles ($n=5$). Asterisks (**) indicated statistical significance <0.01 (t test)

experiment, which is similar to what Ralph et al. (2007) observed when natural sea-ice algal communities were exposed to different salinities. At the same time, both fatty acid and TBARS content increased considerably in

the salinity 10 treatment. It is possible that *N. lecointei* accumulate energy-rich storage products when exposed to unfavorable conditions that limits growth as long as the carbon supply exceeds the photosynthetic capacity of the cells, similar to that observed in the eustigmatophyte *Nannochloropsis* sp. (Pal et al. 2011). It is also possible that cell lysis from the hypoosmotic shock may have overestimated cellular lipid and MDA content, if particle-bound lipids from cell debris are collected on the filters for TBARS and fatty acid analysis, similar to the way other macromolecules are retained on $0.2 \mu\text{m}$ filters after lysis with H_2SO_4 (Torstensson et al. 2019).

Studies focusing on the freezing aspect of sea ice have shown that increased salinity reduces growth rates in sea-ice diatoms, and that they can become more tolerant to hyperosmotic conditions as the temperature decreases (Aletsee and Jahnke 1992; Gleitz and Thomas 1992), highlighting the importance of studying the synergism between environmental constraints on physiological processes. Interestingly, a similar trend also seems to occur at higher temperatures in the present study, as we observed a statistically significant interaction between temperature and salinity on the growth of *N. lecointei*. Although this interaction could not be fully described using a multiple comparison test, it is likely that the significant interaction originated from the slightly higher growth at 3°C and salinity 20, suggesting that *N. lecointei* grows faster at intermediate salinities when temperature is also higher than in the sea-ice environment. Our growth rate data also suggest that the optimal growth salinity for *N. lecointei* is somewhere within the range of 20–35. This range is lower than the average salinity in the Southern Ocean, but similar to that Antarctic sea-ice algae may experience in the summer (Torstensson et al. 2018) and close to the optimal salinity of the Antarctic sea-ice diatom *Navicula* cf. *normaloides* (Schlie and Karsten 2016). Our data suggest that *N. lecointei* may be adapted to a lower salinity than the underlying seawater, and may have a competitive advantage as the sea ice becomes associated with features related to ice melt, which may explain its high relative abundance in sea ice going through melting stages (Ligowski 1992).

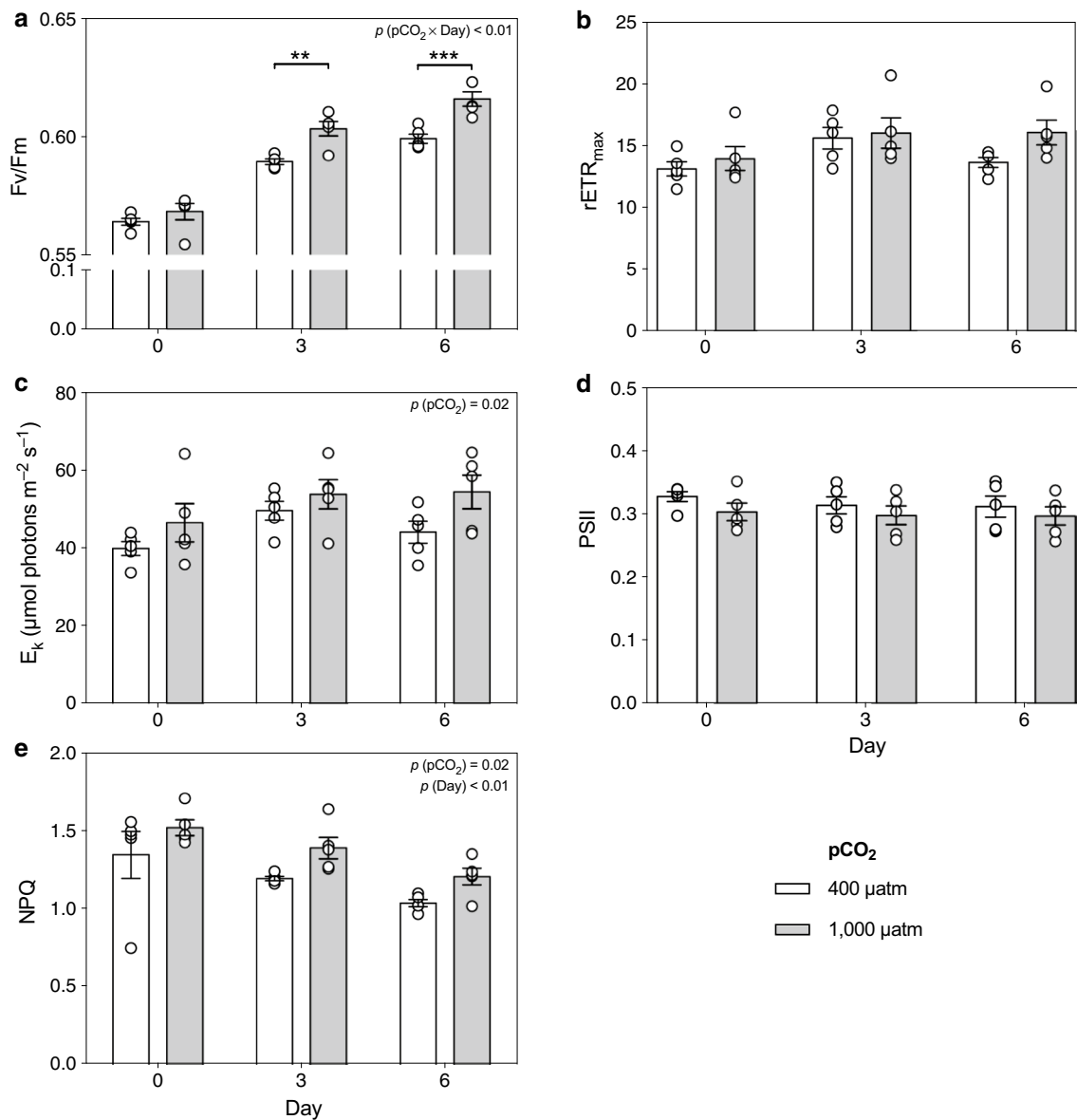


Fig. 6 Variable fluorescence parameters in *Nitzschia lecontei* after 6 days of exposure to two pCO₂. Parameters included are **a** maximum quantum yield of PSII (F_v/F_m), **b** maximum relative electron transport rate ($rETR_{max}$), **c** light saturation point (E_k), **d** PSII efficiency (α_{PSII}) and **e** non-photochemical quenching (NPQ). Error bars repre-

sent standard error and the individual values are displayed with open circles ($n=5$). Asterisks denote statistical significance of $p < 0.01$ and $p < 0.001$ (** and ***, respectively, Tukey's test) where a significant interaction was present (**a**)

No or very minor negative effects of increased pCO₂ have previously been reported on the growth of *N. lecontei* at -1.8 °C (Torstensson et al. 2013, 2015b), which is consistent with this study. By the end of the experiment in the present study, however, we observed a 16% increase in NPQ and a 14% increase in TBARS content at high compared to low pCO₂, indicating that ocean acidification may lead to higher PAR sensitivity in *N. lecontei*, similar to that seen in natural sea-ice algal assemblages (Castrisios et al. 2018) and in mesophilic diatoms (Gao et al. 2012). Radiation

stress can be coupled with increased lipid peroxidation in Antarctic microalgae (Buma et al. 2006), which may have been coupled with a mismatch in PSII efficiency and reactive oxygen species scavenging as a result of lowered medium pH. Increased levels of oxidative stress may also explain why *N. lecontei* grew slower and experienced more leakage of dissolved organic carbon (DOC) as a stress response when exposed to high pCO₂ for up to 194 days (Torstensson et al. 2015b). Although cells had higher TBARS content at high pCO₂, neither growth nor fatty acid composition were

affected, suggesting that the diatom was capable of protecting itself from this seemingly minor stress.

Elevated $p\text{CO}_2$ has in previous studies resulted in increased release of dissolved organic carbon due to carbon overconsumption in microalgae when inorganic nutrient balances are shifted towards a more carbon-rich state, which may also affect the bacterial component of polar marine systems (Engel et al. 2013; Torstensson et al. 2015b). Extracellular polysaccharide substances (EPS) are carbon-rich compounds produced by microorganisms and play an important role in sea-ice environments (Deming and Young 2017). Yields of EPS have been reported to increase in sea-ice diatoms when grown at elevated salinity and decreased temperature, and are therefore believed to act as important osmo- and cryoprotectant (Aslam et al. 2012; Torstensson et al. 2019). The cryoprotective properties of EPS may explain why the carbohydrate content of *N. lecointei* was higher at $-1.8\text{ }^\circ\text{C}$ compared to $3\text{ }^\circ\text{C}$ in the present study. In addition, the production of the uronic acid component of EPS has previously been shown to increase in temperate biofilms exposed to high $p\text{CO}_2$ (Lidbury et al. 2012). However, we did not observe any effects of enhanced carbohydrate accumulation at high $p\text{CO}_2$, which could be used as a proxy for particulate EPS production, although the DOC fraction is unknown in the present study and may represent a noticeable part of the excreted carbon in this diatom strain (Torstensson et al. 2015b).

According to our data, the higher temperature (3°) and the intermediate salinity (20) treatments resulted in optimal growth conditions for *N. lecointei*, as carbohydrate and fatty acid accumulation was lower, and protein synthesis was higher (coinciding with high growth rate); in addition, saturated fatty acids were also higher at low temperate and low salinity, as well as TBARS content. All these data indicate higher stress at low temperature and low salinity, thus the metabolism was directed to the synthesis and accumulation of carbohydrates and fatty acids. In comparison to ocean warming and desalination, ocean acidification had limited effects on the physiology and biochemical composition of *N. lecointei*. Although the outcome of ocean acidification experiments on sea-ice algae have been mixed with positive, negative and neutral effects, the effect sizes have been relatively small compared to other environmental stresses, such as temperature (Aletsee and Jahnke 1992; Gleitz and Thomas 1992; McMinn 2017). Psychrophilic diatoms maintain efficient carbon concentrating mechanisms (CCMs) and high concentrations of Rubisco (Tortell et al. 2013; Trimborn et al. 2013; Young et al. 2015a). It is also likely that the investments in CCMs are less costly at low temperatures due to the high solubility of CO_2 (Young et al. 2015b), which may explain why *N. lecointei* was only affected by ocean acidification at elevated temperature in a previous experiment (Torstensson et al. 2013). Although most ocean

acidification experiments on sea-ice microorganisms have been performed using short incubation times (McMinn 2017), it is important to consider the duration of the experiment when interpreting these results, as some effects of increased $p\text{CO}_2$ may not be detected in sea-ice diatoms until after a long acclimation period (Torstensson et al. 2015b). In addition, sea ice is an environment with high seasonal $p\text{CO}_2$ dynamics (Geilfus et al. 2012), suggesting that the microorganisms inhabiting this environment are used to tolerate large variations in pH and therefore less likely to be negatively affected by a 0.4-unit decrease. Therefore, we conclude that the physicochemical changes related to sea ice melting have greater consequences than the direct effects of future ocean acidification (from 400 to $1000\text{ }\mu\text{atm } p\text{CO}_2$) on *N. lecointei*.

Acknowledgements Open access funding provided by Uppsala University. This study was funded by a fellowship from the Campus de Excelencia Internacional del Mar (CEIMAR). Additional support was provided by the Royal Society of Arts and Sciences in Gothenburg (KVVS), Ymer –80 Foundation and Helge Ax:son Johnson's Foundation. C.J. was financed by project CGL2015-67014-R of the Spanish Ministry of Economy and Competitiveness. We thank Dr. Ken Ryan and two anonymous reviewers for their helpful comments on the manuscript.

Compliance with ethical standards

Conflict of interest The authors declare they have no conflicts of interest regarding this work.

Open Access This article is distributed under the terms of the Creative Commons Attribution 4.0 International License (<http://creativecommons.org/licenses/by/4.0/>), which permits unrestricted use, distribution, and reproduction in any medium, provided you give appropriate credit to the original author(s) and the source, provide a link to the Creative Commons license, and indicate if changes were made.

References

- Aletsee L, Jahnke J (1992) Growth and productivity of the psychrophilic marine diatoms *Thalassiosira antarctica* Comber and *Nitzschia frigida* Grunow in batch cultures at temperatures below the freezing point of sea water. *Polar Biol* 11:643–647
- Arrigo KR (2017) Sea ice as a habitat for primary producers. In: Thomas DN (ed) *Sea Ice*. Wiley, Chichester, pp 352–370
- Arrigo KR, Thomas DN (2004) Large scale importance of sea ice biology in the Southern Ocean. *Antarct Sci* 16:471–486
- Arrigo KR et al (2012) Massive phytoplankton blooms under Arctic sea ice. *Science* 336:1408
- Arrigo K, Worthen DL, Dixon PL, Lizotte MP (2013) Primary productivity of near surface communities within Antarctic pack ice. In: Lizotte MP, Arrigo KR (eds) *Antarctic sea ice: biological processes, interactions and variability*. American Geophysical Union, Washington, pp 23–43.
- Aslam SN, Cresswell-Maynard T, Thomas DN, Underwood GJC (2012) Production and characterization of the intra- and extracellular carbohydrates and polymeric substances (EPS) of three

- sea-ice diatom species, and evidence for a cryoprotective role for EPS. *J Phycol* 48:1494–1509
- Assmy P et al (2013) Floating ice-algal aggregates below melting Arctic sea ice. *PLoS ONE* 8:e76599. <https://doi.org/10.1371/journal.pone.0076599>
- Buma AGJ, Wright SW, van den Eenden RL, van de Poll WH, Davidson AT (2006) PAR acclimation and UVBR-induced DNA damage in Antarctic marine microalgae. *Mar Ecol Prog Ser* 315:33–42
- Castrisios K, Martin A, Müller MN, Kennedy F, McMinn A, Ryan KG (2018) Response of Antarctic sea-ice algae to an experimental decrease in pH: a preliminary analysis from chlorophyll fluorescence imaging of melting ice. *Polar Res* 37:1438696. <https://doi.org/10.1080/17518369.2018.1438696>
- Deming JW, Young JN (2017) The role of exopolysaccharides in microbial adaptation to cold habitats. In: Margesin R (ed) *Psychrophiles: from biodiversity to biotechnology*. Springer International Publishing, Cham, pp 259–284
- Dickson AG (1990) Standard potential of the reaction: $\text{AgCl}(s) + \text{OH}_2(g) = \text{Ag}(s) + \text{HCl}(aq)$, and the standard acidity constant of the ion HSO_4 in synthetic seawater from 273.15 to 318.15 K. *J Chem Thermodyn* 22:113–127
- Dickson AG, Millero FJ (1987) A comparison of the equilibrium constants for the dissociation of carbonic acid in seawater media. *Deep Sea Res Pt I* 34:1733–1743
- Dickson AG, Sabine CL, Christian JR (2007) Guide to best practices for ocean CO_2 measurements. PICES Special Publication, 3, North Pacific Marine Science Organization, 176pp, Sidney, British Columbia
- Eilers PHC, Peeters JCH (1988) A model for the relationship between light intensity and the rate of photosynthesis in phytoplankton. *Ecol Model* 42:199–215
- Engel A, Borchard C, Piontek J, Schulz K, Riebesell U, Bellerby R (2013) CO_2 increases ^{14}C -primary production in an Arctic plankton community. *Biogeosciences* 10:1291–1308
- Fernández-Gómez B et al (2018) Bacterial community structure in a sympagic habitat expanding with global warming: brackish ice brine at 85–90°N. *ISME J* 13:316–333
- Gao K et al (2012) Rising CO_2 and increased light exposure synergistically reduce marine primary productivity. *Nat Clim Chang* 2:519–523
- Geilfus NX et al. (2012) Dynamics of $p\text{CO}_2$ and related air-ice CO_2 fluxes in the Arctic coastal zone (Amundsen Gulf, Beaufort Sea). *J Geophys Res Oceans* 117:C00G10 doi:10.1029/2011JC007118
- Gleitz M, Thomas DN (1992) Physiological responses of a small Antarctic diatom *Chaetoceros* sp. to simulated environmental constraints associated with sea-ice formation. *Mar Ecol Prog Ser* 88:278–287
- Gleitz M, Thomas DN (1993) Variation in phytoplankton standing stock, chemical composition and physiology during sea-ice formation in the southeastern Weddell Sea, Antarctica. *J Exp Mar Biol Ecol* 173:211–230
- Gran G (1952) Determination of the equivalence point in potentiometric titrations. Part II. *Analyst* 77:661–671
- Guillard RRL (1975) Culture of phytoplankton for feeding marine invertebrates. In: Smith WL, Chanley MH (eds) *Culture of marine invertebrate animals*. Plenum, New York, pp 29–60
- Heath RL, Packer L (1968) Photoperoxidation in isolated chloroplasts: I. Kinetics and stoichiometry of fatty acid peroxidation. *Arch Biochem Biophys* 125:189–198
- Hoegh-Guldberg O, Bruno JF (2010) The impact of climate change on the world's marine ecosystems. *Science* 328:1523–1528
- Horner R, Schrader GC (1982) Relative contributions of ice algae, phytoplankton, and benthic microalgae to primary production in nearshore regions of the Beaufort Sea. *Arctic* 35:485–503
- IPCC (2013) *Climate change 2013: The physical science basis. Contribution of working group I to the fifth assessment report of the Intergovernmental Panel on Climate Change*. In: Stocker TF et al. (eds). Cambridge University Press, Cambridge
- Kahm M, Hasenbrink G, Lichtenberg-Fraité H, Ludwig J, Kschischko M (2010) grofit: fitting biological growth curves with R. *J Stat Softw* 33:1–21
- Kates M, Volcani BE (1966) Lipid components of diatoms. *Biochim Biophys Acta Lipids Lipid Metab* 116:264–278
- Kochert A (1978) Carbohydrate determination by the phenol sulfuric acid method. In: Hellebust JA, Craigie JS (eds) *Handbook of phycological methods: physiological and biochemical methods*. Cambridge University Press, Cambridge, pp 95–97
- Leu E, Wiktor J, Søreide JE, Berge J, Falk-Petersen S (2010) Increased irradiance reduces food quality of sea ice algae. *Mar Ecol Prog Ser* 411:49–60
- Lidbury I, Johnson V, Hall-Spencer JM, Munn CB, Cunliffe M (2012) Community-level response of coastal microbial biofilms to ocean acidification in a natural carbon dioxide vent ecosystem. *Mar Pollut Bull* 64:1063–1066
- Ligowski R (1992) Sea ice diatoms and ice edge planktonic diatoms at the northern limit of the Weddell Sea pack ice. *Proc NIPR Symp Polar Biol* 5:9–20
- Lizotte MP (2001) The contributions of sea ice algae to Antarctic marine primary production. *Am Zool* 41:57–73
- Longhi ML, Schloss IR, Wiencke C (2003) Effect of irradiance and temperature on photosynthesis and growth of two Antarctic benthic diatoms, *Gyrosigma subsalinum* and *Odontella litigiosa*. *Bot Mar* 46:276–284
- Lyon BR, Bennett-Mintz JM, Lee PA, Janech MG, DiTullio GR (2016) Role of dimethylsulfoniopropionate as an osmoprotectant following gradual salinity shifts in the sea-ice diatom *Fragilariopsis cylindrus*. *Environ Chem* 13:181–194
- McMinn A (2017) Reviews and syntheses: ice acidification, the effects of ocean acidification on sea ice microbial communities. *Biogeosciences* 14:3927–3935
- Mehrbach C, Culbertson CH, Hawley JE, Pytkowicz RM (1973) Measurement of the apparent dissociation constants of carbonic acid in seawater at atmospheric pressure. *Limnol Oceanogr* 18:897–907
- Meredith MP, King JC (2005) Rapid climate change in the ocean west of the Antarctic Peninsula during the second half of the 20th century. *Geophys Res Lett* 32:L19604. <https://doi.org/10.1029/2005GL024042>
- Mocking RJT et al (2012) Statistical methodological issues in handling of fatty acid data: percentage or concentration, imputation and indices. *Lipids* 47:541–547
- Nilsson AK et al (2019) Influence of human milk and parenteral lipid emulsions on serum fatty acid profiles in extremely preterm infants. *JPEN J Parenter Enteral Nutr* 43(1):152–161
- Pal D, Khozin-Goldberg I, Cohen Z, Boussiba S (2011) The effect of light, salinity, and nitrogen availability on lipid production by *Nannochloropsis* sp. *Appl Microbiol Biotechnol* 90:1429–1441
- Palmisano AC, Beeler SooHoo J, Sullivan CW (1987) Effects of four environmental variables on photosynthesis-irradiance relationships in Antarctic sea-ice microalgae. *Mar Biol* 94:299–306
- Petzoldt T (2018) growthrates: Estimate Growth Rates from Experimental Data, R package version 0.7.2., <https://CRAN.R-project.org/package=growthrates>
- Pierrot D, Lewis E, Wallace DWR (2006) MS Excel program developed for CO_2 system calculations, Version 2.1, Oak Ridge, Tennessee
- Pinheiro J, Bates D, DebRoy S, Sarkar D, R Core Team (2018) nlme: linear and nonlinear mixed effects models, R package version 3.1–137, <https://CRAN.R-project.org/package=nlme>
- Qu C-F et al (2017) Effects of ocean acidification on the physiological performance and carbon production of the Antarctic sea ice diatom *Nitzschia* sp. *ICE-H Mar Pollut Bull* 120:184–191
- Quinn GP, Keough MJ (2002) *Experimental design and data analysis for biologists*. Cambridge University Press, Cambridge

- R Core Team (2018) R: a language and environment for statistical computing, Version 3.5.1., <https://www.R-project.org/>, R Foundation for Statistical Computing, Vienna, Austria
- Rajanaahally MA, Lester PJ, Convey P (2015) Aspects of resilience of polar sea ice algae to changes in their environment. *Hydrobiologia* 761:261–275
- Ralph PJ, Gademann R (2005) Rapid light curves: a powerful tool to assess photosynthetic activity. *Aquat Bot* 82:222–237
- Ralph PJ, Ryan KG, Martin A, Fenton G (2007) Melting out of sea ice causes greater photosynthetic stress in algae than freezing in. *J Phycol* 43:948–956
- Riaux-Gobin C, Poulin M, Dieckmann GS, Labrune C, Vétion G (2011) Spring phytoplankton onset after the ice break-up and sea-ice signature (Adélie Land, East Antarctica). *Polar Res* 30:5910. <https://doi.org/10.3402/polar.v30i0.5910>
- Ryan KG, Ralph P, McMinn A (2004) Acclimation of Antarctic bottom-ice algal communities to lowered salinities during melting. *Polar Biol* 27:679–686
- Schlie C, Karsten U (2016) Growth of the Antarctic sea ice diatom *Navicula cf. normaloides* Cholnoky at different temperatures and salinities. *Algol Stud* 151–152:39–49
- Smith PK et al (1985) Measurement of protein using bicinchoninic acid. *Anal Biochem* 150:76–85
- Suzuki H, Hulatt CJ, Wijffels RH, Kiron V (2019) Growth and LC-PUFA production of the cold-adapted microalga *Koliella antarctica* in photobioreactors. *J Appl Phycol* 31:981–997
- Teoh M-L, Phang S-M, Chu W-L (2013) Response of Antarctic, temperate, and tropical microalgae to temperature stress. *J Appl Phycol* 25:285–297
- Thomas DN, Dieckmann GS (2002) Antarctic sea ice—a habitat for extremophiles. *Science* 295:641–644
- Torstensson A, Hedblom M, Andersson J, Andersson MX, Wulff A (2013) Synergism between elevated $p\text{CO}_2$ and temperature on the Antarctic sea ice diatom *Nitzschia lecontei*. *Biogeosciences* 10:6391–6401
- Torstensson A, Dinasquet J, Chierici M, Fransson A, Riemann L, Wulff A (2015a) Physicochemical control of bacterial and protist community composition and diversity in Antarctic sea ice. *Environ Microbiol* 17:3868–3881
- Torstensson A, Hedblom M, Mattsdotter Björk M, Chierici M, Wulff A (2015b) Long-term acclimation to elevated $p\text{CO}_2$ alters carbon metabolism and reduces growth in the Antarctic diatom *Nitzschia lecontei*. *Proc R Soc Biol Sci Ser B* 282
- Torstensson A, Fransson A, Currie K, Wulff A, Chierici M (2018) Microalgal photophysiology and macronutrient distribution in summer sea ice in the Amundsen and Ross Seas. *Antarctica PLoS ONE* 13:e0195587. <https://doi.org/10.1371/journal.pone.0195587>
- Torstensson A, Young JN, Carlson LT, Ingalls AE, Deming JW (2019) Use of exogenous glycine betaine and its precursor choline as osmoprotectants in Antarctic sea-ice diatoms. *J Phycol* 55:663–675
- Tortell PD et al (2013) Inorganic C utilization and C isotope fractionation by pelagic and sea ice algal assemblages along the Antarctic continental shelf. *Mar Ecol Prog Ser* 483:47–66
- Trimborn S, Brenneis T, Sweet E, Rost B (2013) Sensitivity of Antarctic phytoplankton species to ocean acidification: Growth, carbon acquisition, and species interaction. *Limnol Oceanogr* 58:997–1007
- van de Poll WH, Alderkamp AC, Janknegt PJ, Roggevald J, Buma AGJ (2006) Photoacclimation modulates excessive photosynthetically active and ultraviolet radiation effects in a temperate and an Antarctic marine diatom. *Limnol Oceanogr* 51:1239–1248
- Wulff A, Iken K, Quartino ML, Al-Handal A, Wiencke C, Clayton MN (2009) Biodiversity, biogeography and zonation of marine benthic micro- and macroalgae in the Arctic and Antarctic. *Bot Mar* 52:491–507
- Young JN, Goldman JAL, Kranz SA, Tortell PD, Morel FMM (2015a) Slow carboxylation of Rubisco constrains the rate of carbon fixation during Antarctic phytoplankton blooms. *New Phytol* 205:172–181
- Young JN, Kranz SA, Goldman JAL, Tortell PD, Morel FMM (2015b) Antarctic phytoplankton down-regulate their carbon-concentrating mechanisms under high CO_2 with no change in growth rates. *Mar Ecol Prog Ser* 532:13–28
- Zhang Q, Gradinger R, Spindler M (1999) Experimental study on the effect of salinity on growth rates of Arctic-sea-ice algae from the Greenland Sea. *Boreal Environ Res* 4:1–8

Publisher's Note Springer Nature remains neutral with regard to jurisdictional claims in published maps and institutional affiliations.